Sensors & Transducers, Vol. 162 , Issue 1, January 2014, pp. 42-46

www.sensorsportal.com

Sensors & Transducers

http://www.sensorsportal.com

Studies of the Synchronous Sensing Method in the Microfluidic Cell Impedance Detection

[1] Jie DAI, [2] Yuhwa LO, [1] Kecheng YANG

[1] School of Optical and Electronic information, Huazhong University of Science and Technology, Wuhan 430074, China

[2] Department of Electrical and Computer Engineering, University of California at San Diego, La Jolla, CA, 92093-0407, United States of America

E-mail: kcyang@mail.hust.edu.cn

Received: 21 October 2013 /Accepted: 9 January 2014 /Published: 31 January 2014

Abstract: Microfluidic impedance sensors play a significant role in point-of-care applications, clinical tests and laboratory studies. Instead of the traditional signal process method with the envelope detector, filter banks and multistage amplifier, we have reported a new implement using synchronous sampling and orthogonal detecting. By studying the intensity and phase modulation in the cell impedance sensing progress, we have calculated the SNR of the new method compare with the raw data. Base on the physical model and the calculation, we have demonstrated a simulation result which shows a capability to detect the signal of 1um cell in a noisy environment. *Copyright © 2014 IFSA Publishing, S. L.*

Keywords: Phase, Orthogonal wave, Multiply-add operation, Noise inhibition, Synchronous sampling.

1. Introduction

Microfluidic cell counters provide us powerful implements to point-of-care applications, clinical tests and laboratory studies [1, 2]. Compare to other cell detecting means with optical, acoustic and magnetic sensors, it is widely used since it's low cost, label-free and easy to use [3-6].

Cell impedance has been studied by the cell counter researchers for years because it's directly related to the cell size. By analyzing the response to DC/AC motivations, variant physical models and detecting methods have been developed [7-11]. For example, Gawad group has built an accurate microfluidic-electric model by inducing the frequency-permittivity bonding and geometric factor correction [12, 13]. Plenty of microfluidic impedance counters focuses on the signal intensity measurement were invented in recent years. Zhe Mei et al. reported an electrode design which can produced a uniform electric field and detected 7um cell with high resolution and low CV [14]. However, those devices suffered from the background noise which covered the weak signal of small cells. It's difficult, if not impossible, to make a post process circuit which can filter, amplify and recover the signal from a very small cell in the real application since it attenuates with the third power of the cell diameter. Also, the throughput range of the device is limited because the pass window of the filter bank on the PCB board cannot automatically fix to the cell signal with fluctuant frequency when the flow velocity changes.

We reported a new signal process method based on the physical model of impedance measurement by using synchronous sampling and orthogonal detecting. The SNR of the signal is largely increased for cells with variant diameter without any envelope detector, filter banks or multistage amplifier. With this method, it gives more probability to measure small cells like platelet or bacterial in practical environment.

Article number P_1747

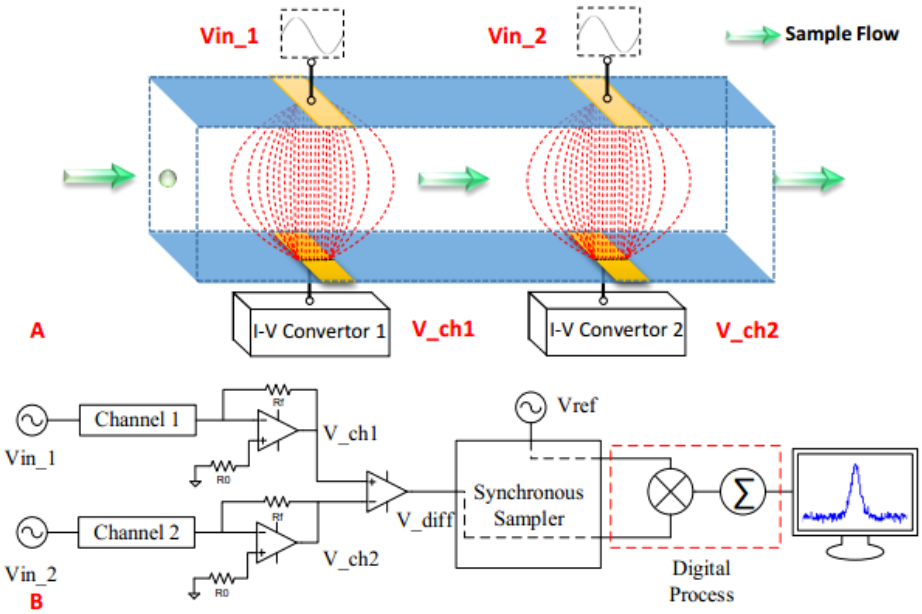

Fig. 1. The Device Structure, Operation Principle and Signal Processing Diagram. (a) The demonstration of the sensor structure. The yellow rectangle pads are the surface electrodes. The red dash lines are the electric field lines. The green arrow shows the flow direction of the cell sample. The green sphere represents a cell entering the sensing area. The Vin_1 and Vin_2 indicate two separate motivation waves which are input into Channel 1 and 2. The V_ch1 and V_ch2 are the related voltage signal from the I-V convertor 1 and 2. (b) The signal processing flow. The differential amplifier between the I-V convertor and the Synchronous Sampler produces the difference of V_ch1 and V_ch2. The output and the reference wave are sampled simultaneously, processed and displayed on the screen.

2. Results

2.1. System Design and Work Flow

The design and work flow of a dual-channel micro Culter counter is shown in Fig. 1. In this model, two typical electric impedance [10] sensors were integrated into a microfluidic channel (Fig. 1(a)). Two sine-wave voltages (Vin_1 and Vin_2) were separately applied to each surface electrode pairs placed face to face on the channel floor and ceiling. When the conductive solution fulfilled the sensing area between electrodes, an electric field was built to measure the impedance of the sample flow. The green arrow indicates the direction of cell suspension infused into the micro channel. Once a cell passing through the detection channel 1 (the left electrode pair), it slightly changed the impedance of this sensing area without disturbing the channel 2 (the right electrode pair). For a stable input voltage, the current of each channel was modulated by the target cell obeying Ohm's law. This modulation will be received and processed by the external electronics after being converted to voltage signal.

Unlike most of the present design which enhanced the raw signal from the impedance sensor with envelope detectors, filter banks and multistage amplifiers [14], a novel method based on the physical model is reported here with high resolution and sensitivity, especially in small cells or particles. Fig. 1(b) indicates the structure of the whole system including the post data processing. The signal V_ch1 and V_ch2 were generated by the inverting amplifier circuit when a cell ran through sensors. To raise the SNR, a differential amplifier was applied to inhibit the common noise. The output signal V_{diff} was sampled by a high speed synchronous sampler and turned to a digital signal. Meanwhile, a reference wave V_{ref} which was orthogonal to Vin_1 and Vin_2 was also induced into the sampler. These two data streams were multiplied, then accumulated by a digital processor which also displayed the data on screen.

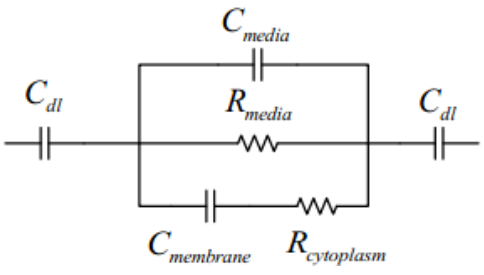

Fig. 2. The equivalent model of an impedance sensor.

2.2. Principle of Methods

In the case of the classic Culter counter, several equivalent models were raised up to simplify the electric analysis [8, 11, 15]. Fig. 2 is a widely

reported structure which sets the double layer capacitor C_{dl} in tandem with an RC parallel-serial network. In the network, C_{media} and R_{media} are the capacitance and resistance of the environmental media. When the cell displaces the same volume of highly conductive solution (like cell culture media or PBS), it will enlarge the total impedance by inducing the cell membrane capacitor $C_{membrane}$ and the cell cytoplasm resistance $R_{cytoplasm}$. Base on this model, Gawad group has derived the total impedance Z_{total} of the channel which the cell registered to [12, 13]. Considering the geometry factor and the frequency modulated permittivity, Z_{total} can be expressed as [13]:

$$Z_{total} = \frac{1}{j\omega C_{dl}} + R_{media}(1 + j\omega C_{membrane})[j\omega R_{media} C_{membrane} + (1 + j\omega R_{cytoplasm} C_{membrane})(1+j\omega R_{media} C_{media})]^{-1} \quad (1)$$

The parameters in equation (1) can be derived by using Maxwell' mixture theory and the Schwarz-Christoffel mapping. According to the circuit design, the output of I-V convertor is:

$$V_{out1} = \frac{R_f}{Z_{total}} Vin\_1 = \frac{R_f V_0}{|Z_{total}|} Cos(\omega t - \varphi_z) \quad (2)$$

where V_{out1} is the output from channel 1 which contains a cell. V_{out2} is the output from the empty channel 2. Fig 3(a) shows the difference of absolute value between the cell signal V_{out1} and the environment signal V_{out2}. The curve rises at low frequency, reaches the top at around 100 kHz to1 MHz depend on the cell size and then goes flat at high frequency. The value decays exponentially with the cell diameter in a wide frequency range. Fig. 3(b) indicates the phase difference between V_{out1} and V_{out2}. Similar to the absolute value, it variance a lot when cell size changes. The current methods generally focused on the signal intensity detection but ignored the phase information. Envelope detector, filter banks and multi-stage amplifier are used to detect the signal envelop, filter the noise and enhance the signal. However, it's too difficult to distinguish the small cell since its initial SNR is too low. To minimize the environment noise, we added a differential circuit which can greatly reduce the common noise. The output of this stage is V_{diff}, which can be described as:

$$V_{diff} = V_{out1} - V_{out1} = |V_{diff}| Cos(\omega t - \varphi_{diff}) \quad (3)$$

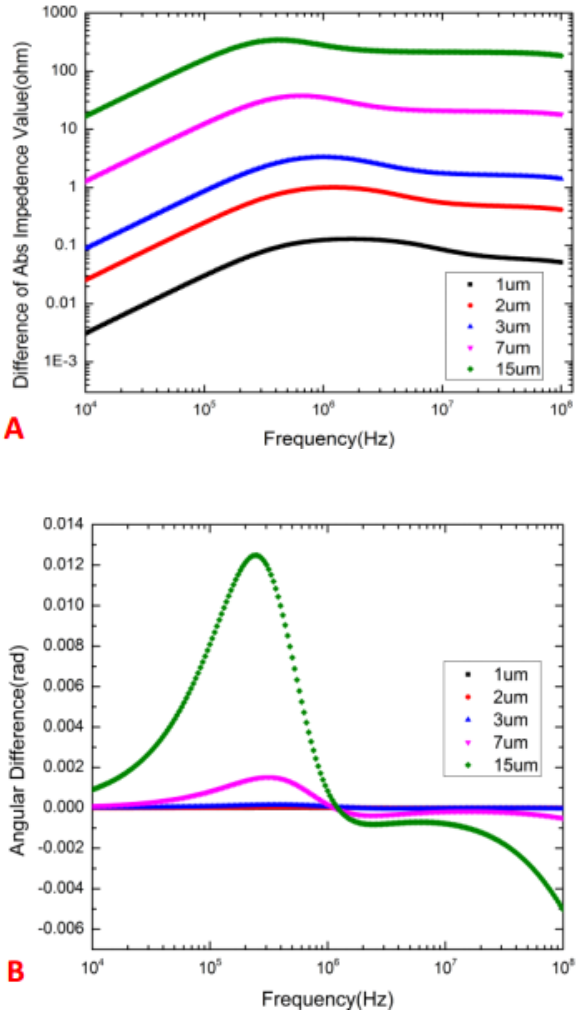

Fig. 3. The raw signal characteristics of the cell with variant sizes versus the frequency. (a) The difference of absolute impedance value between the channels with/without a cell versus the frequency. (b) The angular difference of impedance value between the channels with/without a cell versus the frequency.

We got both intensity and phase signal of V_{diff} by multiplying it with an orthogonal wave V_{ref}, and

$$V_{mul} = V_{diff} \cdot V_{ref} = |V_{diff}| V_0 Cos(\omega t - \varphi_{diff}) Sin(\omega t) = \frac{|V_{diff}| V_0}{2} Sin(2\omega t - \varphi_{diff}) + \frac{|V_{diff}| V_0}{2} Sin(\varphi_{diff}) \quad (4)$$

The first item in the equation (4) is a second harmonic wave which can be removed by accumulation for more than one cycle. The second item is a DC component which can be largely increased while accumulating. Meanwhile, the differential-mode noise N_{diff} which follows the Gaussian white noise distribution will be inhibited. Here, the data SNR after processing was derived compare with the original SNR.

$$SNR_{processed} = \sqrt{\frac{MN}{2}} \frac{Sin(\varphi_{diff}) | V_{diff} |}{\sigma}, \quad (5)$$
$$SNR_{initial} = \frac{| V_{diff} |}{\sigma}$$

where M is the sampling number in each cycle, N is the cycle amount to accumulate, σ is the standard deviation of Gaussian noise N_{diff} before data process. When φ_{diff} is settled, we can greatly enhance the SNR by well setting the factor M and N.

2.3. Simulation Results

Base on the physical model, the geometry and electric parameters were set as below (See Table 1).

The double layer capacitance C_{dl} was 30pF. The flow rate was 15 $\mu L / \min$. Artificial cell impedance was yielded in channel 1. Channel 2 without any cell was kept as the comparison. Two 5 Volts, 500 kHz cosine waves were separately added to the channels. The noise coupled into each channel followed Gaussian distribution $N(0, \sigma^2)$, where $\sigma = 1 \mu V$.

Fig. 4 demonstrates the performance of the simulation result before and after the digital data processing. Here we set M=2000 and N=10. Fig. 4(a), Fig. 4(b), Fig. 4(c) and Fig. 4(d) are the final output intensity with different cell diameter versus the time. The subpanel in each image shows the raw V_{diff} signal. In Fig. 4(a), the SNR of the post processed data is around 3, while the signal of 1 um cell is totally submerged by the noise. Similar results occur in Fig. 4(b) and Fig. 4(c). The raw signal of 2 um cell is still invisible, although the final output is obvious. For 3 um cell, the raw SNR is just around 1. After the multiply-add operation, the signal looks much larger than the background noise. In Fig. 4(d), the noise of raw data is about 300 mV. After the processing, the noise is almost completely removed.

Table 1. Geometry and electric parameters.

Name	Value	Name	Value
Channel Width	50 um	Culture media permittivity	90
Channel Height	50 um	Cytoplasm permittivity	60
Electrode Width	20 um	Culture media conductivity	1.6 S/m
Thickness of cell membrane	5 nm	Cytoplasm conductivity	0.6 S/m
Cell membrane permittivity	11	Cell membrane conductivity	1e-8 S/m

(5)

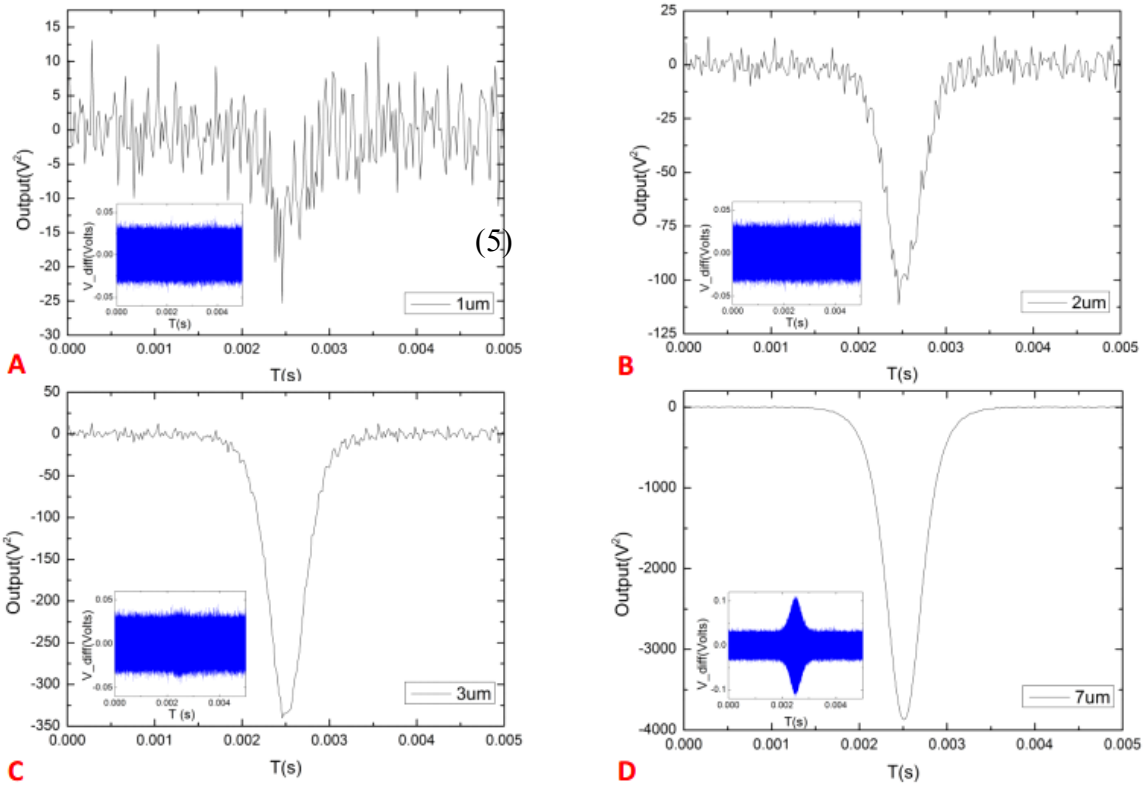

Fig. 4. The performance of the signal process. The 4 big subpanels show the data after a multiply-add operation. These 4 small figures in the down left of each subpanel are the raw data before the digital process. (a), (b), (c) and (d) indicate the signal of the 1 um, 2 um, 3 um and 7 um cells.

3. Conclusions

We have reported a new processing method which can greatly raise the SNR of the single cell counting base on the synchronous sampling and orthogonal detecting. By taking this approach, it's more probable to capture the cell passing event in a noisy environment. Furthermore, it gives a chance to measure the small diameter cell, such as platelet or bacterial, which is difficult to be detected with the traditional post process means. Additionally, this method is simple, highly automatic and easy to operate.

Acknowledgements

Here we thank Mengqi Huang, Hao Liu, Junwei Ye for the great help in the academic discussion. This work is funded by China Scholarship Council.

References

[1]. P. Yager, T. Edwards, E. Fu, et al., Microfluidic diagnostic technologies for global public health, *Nature*, Vol. 442, 2006, pp. 412-418.

[2]. C. D. Chin, V. Linder, S. K. Sia, Lab-on-a-chip devices for global health: past studies and future opportunities, *Lab on a Chip*, Vol. 7, 2007, pp. 41-57.

[3]. D. Ateya, J. Erickson, P. Howell, Jr., et al., The good, the bad, and the tiny: a review of microflow cytometry, *Analytical and Bioanalytical Chemistry*, Vol. 391, 2008, pp. 1485-1498.

[4]. J. Godin, C.-H. Chen, S. H. Cho, et al., Microfluidics and photonics for Bio-System-on-a-Chip: A review of advancements in technology towards a microfluidic flow cytometry chip, *Journal of Biophotonics*, Vol. 1, 2008, pp. 355-376.

[5]. A. Valero, T. Braschler, N. Demierre, et al., A miniaturized continuous dielectrophoretic cell sorter and its applications, *Biomicrofluidics*, Vol. 4, 2010, pp. 022807.

[6]. D. N. Schafer, E. A. Gibson, E. A. Salim, et al., Microfluidic cell counter with embedded opticalfibers fabricated by femtosecond laser ablationand anodic bonding, *Optical Express*, Vol. 17, 2009, pp. 6068-6073.

[7]. K. Cheung, S. Gawad, P. Renaud, Impedance spectroscopy flow cytometry: On-chip label-free cell differentiation, *Cytometry Part A*, Vol. 65A, 2005, pp. 124-132.

[8]. X. Cheng, Y.-S. Liu, D. Irimia, et al., Cell detection and counting through cell lysate impedance spectroscopy in microfluidic devices, *Lab on a Chip*, Vol. 7, 2007, pp. 746-755.

[9]. C. D. Falokun, G. H. Markx, Electrorotation of beads of immobilized cells, *Journal of Electrostatics*, Vol. 65, 2007, pp. 475-482.

[10]. S. Gawad, L. Schild, P. Renaud, Micromachined impedance spectroscopy flow cytometer for cell analysis and particle sizing, *Lab on a Chip*, Vol. 1, 2001, pp. 76-82.

[11]. L. Yang, Y. Li, C. L. Griffis, et al., Interdigitated microelectrode (IME) impedance sensor for the detection of viable Salmonella typhimurium, *Biosensors and Bioelectronics*, Vol. 19, 2004, pp. 1139-1147.

[12]. S. Gawad, K. Cheung, U. Seger, et al., Dielectric spectroscopy in a micromachined flow cytometer: theoretical and practical considerations, *Lab on a Chip*, Vol. 4, 2004, pp. 241-251.

[13]. M. Hywel, S. Tao, H. David, et al., Single cell dielectric spectroscopy, *Journal of Physics D: Applied Physics*, Vol. 40, 2007, pp. 61.

[14]. M. Zhe, C. Sung Hwan, A. Zhang, et al., Counting leukocytes from whole blood using a lab-on-a-chip Coulter counter, in *Proceedings of the IEEE Annual International Conference of the Engineering in Medicine and Biology Society (EMBC'2012)*, 28 August 2012 – 1 September 2012, pp. 6277-6280.

[15]. L. Yang, C. Ruan, Y. Li, Detection of viable Salmonella typhimurium by impedance measurement of electrode capacitance and medium resistance, *Biosensors and Bioelectronics*, Vol. 19, 2003, pp. 495-502.
